Table 1. *Sound velocities in graphite*

See Fig. 11(*b*): $\theta = 88{\cdot}93$ and $\Delta\theta = +1{\cdot}63°$.

00*l*	Δt_{tot} (ms)	t_B (ms)	$\beta(\zeta)$	v_n (km s^{-1})	$c_s(\zeta)$ (km s^{-1})	ζ (°)
004	6·46	83·05	1·693	1·17	1·98	53·7
006	2·78	55·33	1·334	1·75	2·33	41·4
008	1·54	41·50	1·193	2·34	2·79	33·1
0,0,10	0·85	33·19	1·096	2·92	3·20	24·2

Table 2. *Magnitudes of wave vectors, expressed as a fraction of the wave vector for Bragg scattering*

00*l*	q/k_B	$\Delta k_0/k_B$	$\Delta k/k_B$
004	0·070	−0·038	0·080
006	0·085	−0·025	0·088
008	0·104	−0·018	0·106
0,0,10	0·139	−0·012	0·140

In graphite (Bowman & Krumhansl, 1958) the acoustic modes have polarization vectors which are either within the layers ('in-plane modes') or normal to the layers ('out-of-plane modes'). In the present experiment, scattering from the in-plane modes was suppressed by the polarization factor $|\mathbf{Q}.\mathbf{e}(j\mathbf{q})|^2$, and only the out-of-plane modes were observed.

Table 2 gives the magnitudes of q, Δk_0 and Δk at the absorption edge ($\varepsilon = -1$) of the wavelength window, as calculated from the expressions in § 5.

The quantity

$$(\Delta k + \Delta k_0)/2k_B$$

lies between 0·02 and 0·065, so that there is an error of about 4% in the sound velocities quoted in Table 1, which arises from neglecting $(\Delta k + \Delta k_0)$ in (4). In the analysis of the same data by Willis, Carlile, Ward, David & Johnson (1986) this error was eliminated by extrapolating the results to $\Delta\theta = 0$.

Many of the ideas developed in this paper were discussed initially with Dr C. J. Carlile of the Rutherford Appleton Laboratory and with Dr P. Schofield of AERE, Harwell. The experimental measurements were carried out on the pulsed neutron source ISIS of the Rutherford Appleton Laboratory. The author is grateful for the hospitality of Dr C. K. Prout, Head of the Chemical Crystallography Laboratory, Oxford.

References

BOWMAN, J. C. & KRUMHANSL, J. A. (1958). *J. Phys. Chem. Solids*, **6**, 367-379.
ELLIOTT, R. J. & LOWDE, R. D. (1955). *Proc. R. Soc. London. Ser. A*, **230**, 46-73.
JOHNSON, M. W. & DAVID, W. I. F. (1985). Rutherford Appleton Lab. Rep. RAL-85-112.
SEEGER, R. J. & TELLER, E. (1942). *Phys. Rev.* **62**, 37-40.
STEICHELE, E. & ARNOLD, P. (1973). *Phys. Lett. A*, **44**, 165-166.
VAN HOVE, L. (1953). *Phys. Rev.* **89**, 1189-1193.
WILLIS, B. T. M., CARLILE, C. J., WARD, R. C., DAVID, W. I. F. & JOHNSON, M. W. (1986). *Europhys. Lett.* In the press.
WILLIS, B. T. M. & PRYOR, A. W. (1975). *Thermal Vibrations in Crystallography*. Cambridge Univ. Press.

Acta Cryst. (1986). A**42**, 525-533

A New Approach to Multibeam X-ray Diffraction Using Perturbation Theory of Scattering

BY QUN SHEN

Department of Physics, Purdue University, West Lafayette, Indiana 47907, *USA*

(*Received* 8 *March* 1986; *accepted* 23 *May* 1986)

Abstract

Perturbations to conventional two beam X-ray diffraction arising from multibeam scattering effects have been studied theoretically. A simple analytical expression for the diffracted wave field and intensity near a multiple excitation is derived by using the perturbation theory of scattering of electromagnetic waves. Although it cannot be applied to the center of a multibeam diffraction peak, it does show explicitly the asymmetry effect observed in experiments and its phase dependence in the neighborhood of the multibeam point. A numerical calculation for the $\bar{1}1\bar{1}$ *Umweganregung* peak on the almost-forbidden 442 reflection of silicon gives excellent agreement with experimental data and exact n-beam computer calculations based on conventional dynamical theory. From the analytical expression, a simple rule is derived for phase determination in centrosymmetric crystals. A general 'pseudo-four-beam' case where no asymmetry effect exists is also discussed as another example of the applications.

0108-7673/86/060525-09$01.50

Introduction

It has been known in X-ray crystallography that phase information can be partially extracted from multiple-scattering effects (Colella, 1974), especially from the asymmetric pattern of the diffracted intensities near a multibeam point both in the Laue case (Post, 1977) and, more recently, in the Bragg case, where the effect has been observed far from the excitation point and has been called 'virtual Bragg scattering' (Chapman, Yoder & Colella, 1981). Based on this idea, more experiments have been done either to demonstrate the applicability of this method (Gong & Post, 1983; Tischler, Shen & Colella, 1985) or to use this method to determine some unknown phases in centrosymmetric crystals (Schmidt & Colella, 1985).

Multibeam effects are fully explainable using conventional dynamical theory, but in order to do quantitative analyses a computer program is usually required that involves solving an eigenvalue equation for the multi-Bragg-beams (Colella, 1974). Recently some efforts have been made to obtain an approximate solution to the dynamical eigen equation for a three-beam case, treating the third reciprocal node as a perturbation (Juretschke, 1982, 1984; Høier & Marthinsen, 1983; Hümmer & Billy, 1986).

In this report, a new way to attack the multibeam problem will be presented, based on the same perturbation idea but with a different approach. This method is similar to the Born approximation in quantum scattering theory. Since it deals with wave fields directly, rather than seeking first the equation of the dispersion surface, it eliminates the need for component equations and diffraction geometries before getting the final results. The final expression for the wave field is in a simple vector form that contains a summation over all the perturbing reciprocal nodes, which is analogous to the expression for a perturbed wavefunction in quantum mechanics. Since X-ray scattering has never been treated in this way before, the derivation will be given in some detail below.

General formalism

The principle of the perturbation approach has been described in § 9.7 of Jackson's (1974) book *Classical Electrodynamics*, most of which will be repeated below for the completeness of this paper. Two conventions are used that need to be clarified: (1) in order to agree with most expressions in X-ray crystallography, a plane wave will be written as $\exp(-i\mathbf{k}\cdot\mathbf{x}+i\omega t)$ instead of $\exp(i\mathbf{k}\cdot\mathbf{x}-i\omega t)$ as in Jackson's book; (2) for convenience, the magnitude of a wavevector $\mathbf{k}$ is defined as $2\pi/\lambda$ instead of $1/\lambda$. This will not, however, affect the final results.

A general situation of X-ray diffraction can be described as follows: a plane wave

$$\mathbf{D}_0(\mathbf{x}) = \mathbf{D}_0 \exp(-i\mathbf{k}_0\cdot\mathbf{x})$$

with an incident wavevector $\mathbf{k}_0$ is impinging on a crystal that occupies a certain region in free space. What we are looking for is the elastically scattered wave field along an arbitrary direction $\hat{\mathbf{n}}$.

The physical system can be characterized by its dielectric constant function

$$\varepsilon(\mathbf{x}) = \varepsilon_0 + \delta\varepsilon(\mathbf{x}), \tag{1}$$

where $\varepsilon_0 = 1$ and

$$\delta\varepsilon(\mathbf{x}) = \begin{cases} 0 & \text{outside crystal} \\ \psi(\mathbf{x}) & \text{inside crystal} \end{cases} \tag{2}$$

is the deviation from ε_0. $\psi(\mathbf{x})$ is a function proportional to the electronic charge density which can be expanded in a Fourier series with coefficients F_H, the structure factors of the crystal (Batterman & Cole, 1964):

$$\psi(\mathbf{x}) = -\Gamma \sum_H F_H \exp(-i\mathbf{H}\cdot\mathbf{x}). \tag{3}$$

Here the subscript H stands for h, k, l, the Miller indices, and Γ is a constant involving the wavelength λ of the radiation, the unit-cell volume V_c and the classical radius of an electron $r_e = 2{\cdot}818\times10^{-13}$ cm:

$$\Gamma = r_e\lambda^2/\pi V_c. \tag{4}$$

From Maxwell's equations, assuming a single-frequency response from the crystal (elastic scattering), it is not difficult to obtain the following equation for the electric field $\mathbf{E}$ and the displacement vector $\mathbf{D}$:

$$(\nabla^2 + k_0^2)\mathbf{D} = -\nabla\times\nabla\times(\mathbf{D} - \varepsilon_0\mathbf{E}), \tag{5}$$

where the magnetic interaction between the X-rays and the crystal has been neglected. The connection between $\mathbf{D}$ and $\mathbf{E}$ is, as usual, through the dielectric function:

$$\mathbf{D}(\mathbf{x}) = \varepsilon(\mathbf{x})\mathbf{E}(\mathbf{x}) = [\varepsilon_0 + \delta\varepsilon(\mathbf{x})]\mathbf{E}(\mathbf{x}).$$

The deviation $\delta\varepsilon$ is much smaller than ε_0 since $\Gamma \simeq 10^{-7}$ for a common X-ray case. Hence the relation between $\mathbf{D}$ and $\mathbf{E}$ can be approximated as

$$\mathbf{D} - \varepsilon_0\mathbf{E} \simeq (\delta\varepsilon/\varepsilon_0)\mathbf{D},$$

where terms involving the second or higher orders in $\delta\varepsilon$ have been omitted, and (5) becomes ($\varepsilon_0 = 1$)

$$(\nabla^2 + k_0^2)\mathbf{D} = -\nabla\times\nabla\times(\delta\varepsilon\mathbf{D}). \tag{6}$$

A formal solution to (6) can be obtained by using the Green's function method, if the right-hand side is taken as known (Jackson, 1974):

$$\mathbf{D}(\mathbf{x}) = \mathbf{D}^{(0)}(\mathbf{x}) + \frac{1}{4\pi}\int d^3x'\{\exp(-ik_0|\mathbf{x}-\mathbf{x}'|)/|\mathbf{x}-\mathbf{x}'| \times\nabla'\times\nabla'\times[\delta\epsilon(\mathbf{x}')\mathbf{D}(\mathbf{x}')]\}, \tag{7}$$

where $\mathbf{D}^{(0)}$ denotes the solution of the unperturbed

problem, which is just the incident wave:

$$\mathbf{D}^{(0)}(\mathbf{x}) = \mathbf{D}_0 \exp(-i\mathbf{k}_0 \cdot \mathbf{x}). \quad (8)$$

By using (2), the integral region in (7) can be reduced to V, the volume of the crystal. Hence

$$\mathbf{D}(\mathbf{x}) = \mathbf{D}^{(0)}(\mathbf{x}) + \frac{1}{4\pi}\int_V d^3x' \{\exp(-ik_0|\mathbf{x}-\mathbf{x}'|)/|\mathbf{x}-\mathbf{x}'| \times \nabla' \times \nabla' \times [\psi(\mathbf{x}')\mathbf{D}(\mathbf{x}')]\}. \quad (9)$$

This integral equation for $\mathbf{D}$ provides a systematic scheme of successive approximations, similar to the Born approximation in quantum mechanics. In the first-order approximation, $\mathbf{D}(\mathbf{x}')$ in the integrand can be substituted by $\mathbf{D}^{(0)}$, then (9) gives an improved solution for $\mathbf{D}$, beyond $\mathbf{D}^{(0)}$. This improved solution, in turn, can be used in the integrand to give a second-order solution to $\mathbf{D}$, and so on. Therefore we can write the solution to (9) in the form

$$\mathbf{D} = \mathbf{D}^{(0)} + \mathbf{D}^{(1)} + \mathbf{D}^{(2)} + \cdots,$$

where $\mathbf{D}^{(i)}(i = 1, 2, \ldots)$ is the ith-order iteration correction to the unperturbed wave field $\mathbf{D}^{(0)}$. It turns out that $\mathbf{D}^{(1)}$ will represent the two-beam diffraction in the usual kinematic theory and $\mathbf{D}^{(i)}(i \geq 2)$ will represent the multibeam perturbations, with $\mathbf{D}^{(2)}$ involving one intermediate state, $\mathbf{D}^{(3)}$ involving two intermediate states, and so on. In this paper, only $\mathbf{D}^{(1)}$ and $\mathbf{D}^{(2)}$ will be discussed.

First-order solution

To get the first-order correction $\mathbf{D}^{(1)}$, we approximate $\mathbf{D}(\mathbf{x}')$ to $\mathbf{D}^{(0)}(\mathbf{x}')$ in the integrand of (9):

$$\mathbf{D}^{(1)}(\mathbf{x}) = \frac{1}{4\pi}\int_V d^3x' \{\exp(-ik_0|\mathbf{x}-\mathbf{x}'|)/|\mathbf{x}-\mathbf{x}'| \times \nabla' \times \nabla' \times [\psi(\mathbf{x}')\mathbf{D}_0 \exp(-i\mathbf{k}_0 \cdot \mathbf{x}')]\}. \quad (10)$$

Since the observation point $\mathbf{x}$ is usually far away from the localized region where the scattering occurs, *i.e.* $|\mathbf{x}| \gg |\mathbf{x}'|$, we can have the result that

$$|\mathbf{x}-\mathbf{x}'| \simeq r - \hat{\mathbf{n}} \cdot \mathbf{x}', \quad (11)$$

where $\hat{\mathbf{n}}$ is the unit vector along $\mathbf{x}$ and $r = |\mathbf{x}|$. Using this approximation, (10) becomes

$$\mathbf{D}^{(1)}(\mathbf{x}) = \frac{\exp(-ik_0 r)}{4\pi r}\int_V d^3x' \{\exp(ik_0\hat{\mathbf{n}} \cdot \mathbf{x}') \times \nabla' \times \nabla' \times [\psi(\mathbf{x}')\mathbf{D}_0 \exp(-i\mathbf{k}_0 \cdot \mathbf{x}')]\}.$$

Integrating by parts twice, ignoring the surface integrals, which means neglecting the surface scattering, and using (3), we obtain

$$\mathbf{D}^{(1)}(\mathbf{x}) = \frac{\exp(-ik_0 r)}{4\pi r}\Gamma k_0^2 \hat{\mathbf{n}} \times (\hat{\mathbf{n}} \times \mathbf{D}_0) \times \sum_H F_H \int_V d^3x' \exp[i(k_0\hat{\mathbf{n}} - \mathbf{k}_0 - \mathbf{H}) \cdot \mathbf{x}'].$$

The integral in the above equation gives V, the volume of the crystal, only when $k_0\hat{\mathbf{n}} - \mathbf{k}_0 - \mathbf{H} = 0$, otherwise it vanishes. Assuming that only one set of atomic planes $\mathbf{H}$ satisfies Bragg's condition (two-beam case)

$$k_0\hat{\mathbf{n}} = \mathbf{k}_0 + \mathbf{H}, \quad (12)$$

we obtain

$$\mathbf{D}^{(1)}(\mathbf{x}) = \frac{\Gamma k_0^2}{4\pi}\frac{\exp(-ik_0 r)}{r}\hat{\mathbf{n}} \times (\hat{\mathbf{n}} \times \mathbf{D}_0) V F_H. \quad (13)$$

Substituting (4) for Γ and $2\pi/\lambda$ for k_0, we can rewrite (13) as

$$\mathbf{D}^{(1)}(\mathbf{x}) = N r_e F_H \hat{\mathbf{n}} \times (\hat{\mathbf{n}} \times \mathbf{D}_0) \exp(-ik_0 r)/r, \quad (14)$$

where $N = V/V_c$ is the number of unit cells inside the crystal. It is not difficult to realize that (14) gives the diffracted wave field in the usual two-beam case. For a perpendicular-polarized incident beam $\mathbf{D}_0 = D_0\hat{\boldsymbol{\sigma}}_0$, we have

$$\hat{\mathbf{n}} \times (\hat{\mathbf{n}} \times \hat{\boldsymbol{\sigma}}_0) = -\hat{\boldsymbol{\sigma}},$$

and for a parallel-polarized incident beam $\mathbf{D}_0 = D_0\hat{\boldsymbol{\pi}}_0$, we have

$$\hat{\mathbf{n}} \times (\hat{\mathbf{n}} \times \hat{\boldsymbol{\pi}}_0) = -\cos 2\theta \hat{\boldsymbol{\pi}},$$

where θ is the Bragg angle for $\mathbf{H}$, $\hat{\boldsymbol{\sigma}} = \hat{\boldsymbol{\sigma}}_0$ and $\hat{\boldsymbol{\pi}} = \hat{\mathbf{n}} \times \hat{\boldsymbol{\sigma}}$, as shown in Fig. 1. Therefore, for an unpolarized incident beam, the intensity is

$$I^{(1)} = \mathbf{D}^{(1)} \cdot \mathbf{D}^{(1)*}/D_0^2 = (N^2 r_e^2 |F_H|^2/r^2)(1 + \cos^2 2\theta)/2. \quad (15)$$

This is exactly the expression of the two-beam peak intensity that we usually find in the kinematic theory of X-ray diffraction (*e.g.* Warren, 1969).

Second-order solution

The second-order correction $\mathbf{D}^{(2)}$ is obtained by approximating $\mathbf{D}(\mathbf{x}') = \mathbf{D}^{(1)}(\mathbf{x}')$ in the integrand of (9):

$$\mathbf{D}^{(2)}(\mathbf{x}) = \frac{1}{4\pi}\int_V d^3x' \{\exp(-ik_0|\mathbf{x}-\mathbf{x}'|)/|\mathbf{x}-\mathbf{x}'| \times \nabla' \times \nabla' \times [\psi(\mathbf{x}')\mathbf{D}^{(1)}(\mathbf{x}')]\}.$$

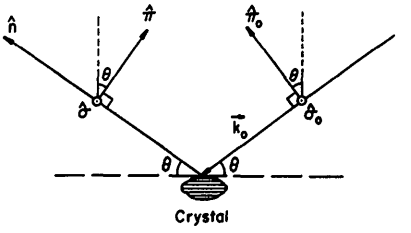

Fig. 1. Illustration of a two-beam diffraction case. $\hat{\boldsymbol{\sigma}} = \hat{\boldsymbol{\sigma}}_0$ are unit vectors normal to the diffraction plane formed by $\mathbf{k}_0$ and $\hat{\mathbf{n}}$. $\hat{\boldsymbol{\pi}} = \hat{\mathbf{n}} \times \hat{\boldsymbol{\sigma}}$ and $\hat{\boldsymbol{\pi}}_0 = \mathbf{k}_0 \times \hat{\boldsymbol{\sigma}}_0/|\mathbf{k}_0|$.

As before, using (11) and integrating by parts twice, we get

$$\mathbf{D}^{(2)}(\mathbf{x}) = -\frac{k_0^2}{4\pi}\frac{\exp(-ik_0 r)}{r}\hat{\mathbf{n}}\times(\hat{\mathbf{n}}\times\mathbf{D}_V), \quad (16)$$

where

$$\mathbf{D}_V \equiv \int_V d^3x' \exp(ik_0\hat{\mathbf{n}}\cdot\mathbf{x}')\psi(\mathbf{x}')\mathbf{D}^{(1)}(\mathbf{x}'). \quad (17)$$

To evaluate this integral, we have to use the original form (10) for $\mathbf{D}^{(1)}(\mathbf{x}')$ instead of (14) which gives $\mathbf{D}^{(1)}$ only at large distances from the crystal. Thus

$$\mathbf{D}_V = \int_V d^3x' \exp(ik_0\hat{\mathbf{n}}\cdot\mathbf{x}')\psi(\mathbf{x}') \times\frac{1}{4\pi}\int_V d^3x''\{\exp(-ik_0|\mathbf{x}'-\mathbf{x}''|)/|\mathbf{x}'-\mathbf{x}''| \times\nabla''\times\nabla''\times[\psi(\mathbf{x}'')\mathbf{D}_0\exp(-i\mathbf{k}_0\cdot\mathbf{x}'')]\}.$$

Using the Fourier expansion (*e.g.* Schiff, 1955)

$$\frac{\exp(-ik_0 r)}{4\pi r} = -\frac{1}{(2\pi)^3}\int d^3k\frac{\exp(-i\mathbf{k}\cdot\mathbf{r})}{k_0^2-k^2},$$

along with (3), we have

$$\mathbf{D}_V = \Gamma^2\sum_G\sum_L F_G F_L\mathbf{k}_L\times(\mathbf{k}_L\times\mathbf{D}_0) \times\int_V d^3x'\exp[i(k_0\hat{\mathbf{n}}-\mathbf{G})\cdot\mathbf{x}'] \times\frac{1}{(2\pi)^3}\int_V d^3x''\exp(-i\mathbf{k}_L\cdot\mathbf{x}'') \times\int d^3k\frac{\exp[-i\mathbf{k}\cdot(\mathbf{x}'-\mathbf{x}'')]}{k_0^2-k^2},$$

where $\mathbf{k}_L = \mathbf{k}_0+\mathbf{L}$, **L** and **G** are reciprocal vectors. The integral over $\mathbf{x}''$ gives a δ function:

$$\frac{1}{(2\pi)^3}\int_V d^3x''\exp[i(\mathbf{k}-\mathbf{k}_L)\cdot\mathbf{x}''] = \delta(\mathbf{k}-\mathbf{k}_L).$$

The integral over **k** can be done easily, so we have

$$D_V = \Gamma^2\sum_G\sum_L F_G F_L\frac{\mathbf{k}_L\times(\mathbf{k}_L\times\mathbf{D}_0)}{k_0^2-k_L^2} \times\int_V d^3x'\exp[i(k_0\hat{\mathbf{n}}-\mathbf{k}_L-\mathbf{G})\cdot\mathbf{x}'].$$

Since we are calculating the correction to the first-order solution, the same Bragg condition (12) should be applied here. Hence the integral

$$\int_V d^3x'\exp[i(k_0\hat{\mathbf{n}}-\mathbf{k}_L-\mathbf{G})\cdot\mathbf{x}'] = \int_V d^3x'\exp[i(\mathbf{H}-\mathbf{L}-\mathbf{G})\cdot\mathbf{x}'] = V\delta_{\mathbf{G},\mathbf{H}-\mathbf{L}}.$$

Therefore the final expression for $\mathbf{D}_V$ is

$$\mathbf{D}_V = \Gamma^2 V\sum_L F_{H-L}F_L\frac{\mathbf{k}_L\times(\mathbf{k}_L\times\mathbf{D}_0)}{k_0^2-k_L^2}. \quad (18)$$

Here the terms **L** = **H** and **O** should be excluded from the summation and **L** should not be exactly on the Ewald sphere since we are considering the perturbations to the two-beam situation.

Substituting (18) into (16), we obtain the second-order correction

$$\mathbf{D}^{(2)}(\mathbf{x}) = -Nr_e\Gamma\frac{\exp(-ik_0 r)}{r}\hat{\mathbf{n}} \times\left[\hat{\mathbf{n}}\times\sum_L F_{H-L}F_L\frac{\mathbf{k}_L\times(\mathbf{k}_L\times\mathbf{D}_0)}{k_0^2-k_L^2}\right]. \quad (19)$$

If (19) is combined with (14), the total diffracted wave field in direction $\hat{\mathbf{n}}$, to second order in Γ, is

$$\mathbf{D}(\mathbf{x}) = Nr_e\frac{\exp(-ik_0 r)}{r}\hat{\mathbf{n}} \times\left\{\hat{\mathbf{n}}\times\left[F_H\mathbf{D}_0-\Gamma\sum_L F_{H-L}F_L\frac{\mathbf{k}_L\times(\mathbf{k}_L\times\mathbf{D}_0)}{k_0^2-k_L^2}\right]\right\}. \quad (20)$$

This expression clearly indicates the multibeam perturbation effects on the conventional two-beam (**O** and **H**) wave field and shows that, to second order in Γ, the effects from different reciprocal nodes are coherently additive. The interactions among different **L** beams in the summation are of higher-order approximations and will be omitted in this paper. The intensity of the diffracted beam in direction $\hat{\mathbf{n}}$ is simply

$$I = \mathbf{D}\cdot\mathbf{D}^*/D_0^2. \quad (21)$$

An explicit expression of the intensity will be given below for a three-beam case.

Discussion

To see the phase dependence of the perturbation effects more clearly, we assume that $F_H \neq 0$ and define

$$\gamma_{HL} = \Gamma|(F_{H-L}F_L)/F_H|$$

and

$$\delta_{HL} = \alpha_{H-L}+\alpha_L-\alpha_H,$$

where the α_H's are the phase angles of F_H's and δ_{HL} is usually called the *invariant phase of the structure-factor triplet* (Post, 1977). Then (20) can be rewritten as

$$\mathbf{D}(\mathbf{x}) = Nr_e F_H\frac{\exp(-ik_0 r)}{r}\hat{\mathbf{n}} \times\left\{\hat{\mathbf{n}}\times\left[\mathbf{D}_0-\sum_L\gamma_{HL}\exp(i\delta_{HL})\frac{\mathbf{k}_L\times(\mathbf{k}_L\times\mathbf{D}_0)}{k_0^2-k_L^2}\right]\right\}. \quad (22)$$

For simplicity, we now consider the three-beam case where only one extra reciprocal node **L** is near the Ewald sphere and we normalize the intensity to

$$I_\perp^H = N^2 r_e^2 |F_H|^2 / r^2,$$

which is the two-beam intensity for a perpendicular-polarized incident beam. From (21), the three-beam intensity in this case is

$$I_\perp = 1 + \gamma_{HL}^2 \frac{(k_L^2 - L_\sigma^2)^2 + (k_{L\pi} L_\sigma)^2}{(k_0^2 - k_L^2)^2} + 2\gamma_{HL} \cos\delta_{HL} \frac{k_L^2 - L_\sigma^2}{k_0^2 - k_L^2}; \quad (23a)$$

and for a parallel polarization,

$$I_\parallel = \cos^2 2\theta + \gamma_{HL}^2 \frac{(k_L^2 \cos 2\theta - k_{L\pi} k_{Ln\pi})^2 + (L_\sigma k_{Ln\pi})^2}{(k_0^2 - k_L^2)^2} + 2\gamma_{HL} \cos\delta_{HL} \frac{k_L^2 \cos 2\theta - k_{L\pi} k_{Ln\pi}}{k_0^2 - k_L^2}, \quad (23b)$$

where $L_\sigma = \mathbf{L} \cdot \hat{\boldsymbol{\sigma}}$, $k_{Ln} = \mathbf{k}_L \cdot \hat{\mathbf{n}}$, $k_{L\pi} = \mathbf{k}_L \cdot \hat{\boldsymbol{\pi}}$, $k_{Ln\pi} = k_{Ln} \sin 2\theta + k_{L\pi} \cos 2\theta$, and $\hat{\boldsymbol{\sigma}}$, $\hat{\boldsymbol{\pi}}$, $\hat{\mathbf{n}}$ are the unit vectors shown in Fig. 1.

These intensity formulae offer a direct visualization of the asymmetry effects observed in experiments, because they are strongly dependent on the sign of $k_0^2 - k_L^2$, which leads to the intensity enhancement and reduction on opposite sides of a three-beam point $k_L = k_0$ (Fig. 2). The strength of the effects depends upon the relative structure factor γ_{HL}, which is expected. Equations (23) also indicate that, besides some geometric factors, the asymmetry is related to the cosine of the invariant phase δ_{HL}, which may cause some less-pronounced effects for non-centrosymmetric crystals. It can also be seen that $I_\perp$ and $I_\parallel$ may have opposite asymmetric patterns since the numerators in the last terms of (23) may have different signs. Hence for optimal asymmetry observations in experiments, a polarized X-ray source would be preferred. Many of the same features were obtained using the perturbation approach in dynamical theory by Juretschke (1982, 1984), Høier & Marthinsen (1983) and Hümmer & Billy (1986).

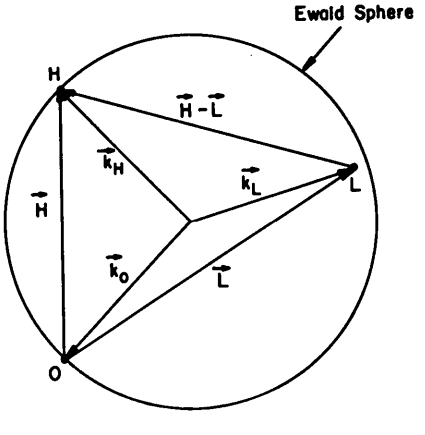

Fig. 2. Illustration of a three-beam diffraction case with the third reciprocal-lattice point **L** close to the Ewald sphere.

It is worth noting that (20) or (22) are basically identical to a wavefunction obtained in first-order perturbation theory in quantum mechanics, with a summation over the nearby states and their energy differences in the denominators. It is owing to this analogy that the asymmetry effects observed in experiments have been called virtual Bragg scattering (VBS) (Chapman, Yoder & Colella, 1981), a concept that comes from virtual transitions or virtual particles in quantum physics.

Equations (20) or (22) yield a general expression for the diffracted wave field that involves no assumptions on the diffraction geometry; neither does it utilize any boundary conditions, so it can be applied to either Bragg or Laue cases and to crystals of any shape. In its derivation, we have neglected absorption and the dynamical effects such as refraction corrections to the wavevectors inside the crystal; therefore it cannot give the Bragg-angle shifts at a multibeam point, *etc.* Neither can it be applied to the center of a multiple reflection peak where the denominator $k_0^2 - k_L^2$ vanishes. In other words, (20) or (22) are basically within the framework of kinematic theory which deals only with single scattering events. By single scattering is meant that an X-ray photon scattered in direction $\hat{\mathbf{n}}$ will not be scattered again. However, with multibeam effects included, (20) or (22) show that the photon may come from different channels, for example, either **O**→**H** or **O**→**L**→**H** (Fig. 2). Hence it proves that the multibeam effect and its phase dependence can be discussed in the framework of single scattering and the asymmetric patterns observed in experiments are purely due to interference among different Bragg beams.

Because of the kinematic nature of the present treatment, the validity of (20) or (22) for strong reflections in perfect crystals is questionable. For weak primary reflections, however, it can provide excellent agreement with experiments in the neighborhood of a multibeam point, as can be seen in the next section.

The fact that (20) or (22) are basically kinematic indicates that the asymmetry effect should also exist in less-perfect crystals, as already seen in experiments (Gong & Post, 1983; Schmidt & Colella, 1985). But whether or not the effects are visible depends on how strong the perturbations are and how mosaic the crystal is, since the mosaic spread may mask the asymmetry.

Applications

Many experimental and theoretical applications can be found for the analytical expression. Three examples are given below.

(1) *Comparison with the* Si 442 *results*:

A recent experiment on the almost-forbidden Si 442 reflection (Tischler, Shen & Colella, 1985) confirmed that the structure factor of 442 changes its phase from negative to positive when the temperature is raised from $T=300$ to $T=700$ K, by comparing the observed reversed asymmetric patterns around the $\bar{1}1\bar{1}$ *Umweganregung* peak with the exact multibeam calculations based on dynamical theory (Colella, 1974), as shown in Figs. 3 and 4. This result has been used for comparison with the present calculations using (20) and (21) since only weak scattering is involved. The same number of beams, which is ten, and the same structure factors, wavelength and lattice parameters have been used as in the exact n-beam computation. The results are shown in Figs. 5 and 6, where the intensities are normalized to the two-beam value. The agreement between the calculations and the experimental data is very good and by comparing Figs. 5 and 6 with Figs. 3 and 4 respectively, one can see that the present calculations are virtually indistinguishable from the exact n-beam dynamical computations. The reason why the dip at $\varphi \simeq 1{\cdot}2°$ in Fig. 3 is not so great as in Fig. 5 is due to the finite experimental resolution and similar considerations in the n-beam computer calculations.

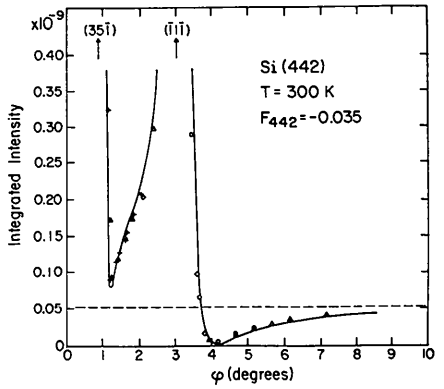

Fig. 3. Integrated intensity (over the angle of incidence) of the Si 442 reflection *vs* φ, the azimuthal angle, as taken from Tischler *et al.* (1985). The dots are experimental data points and the solid curves are ten-beam computer calculations based on dynamical theory. The theoretical two-beam intensity is shown by the dashed line. $T=300$ K, $F_{442}=-0{\cdot}035$.

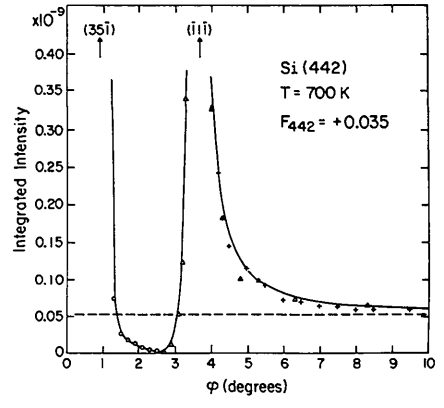

Fig. 4. Same as Fig. 3, except for: $T=700$ K, $F_{442}=+0{\cdot}035$.

The good agreement between Figs. 3 and 4 and 5 and 6 indicates the validity of this perturbation theory and the various approximations involved, at least in the case of virtual Bragg scattering. It also shows that, when normalized to the two-beam value, (21) can be interpreted as an integrated intensity. This is because the two-beam field (14) can be formally transformed to the *modified* two-beam field (20) by simply changing

$$F_H \mathbf{D}_0 \rightarrow F_H \mathbf{D}_0 - \Gamma \sum_L F_{H-L} F_L \frac{\mathbf{k}_L \times (\mathbf{k}_L \times \mathbf{D}_0)}{k_0^2 - k_L^2}.$$

Hence to obtain the integrated intensity, one need only replace the structure factor F_H in a usual two-beam formula by a *modified* structure factor determined by the above transformation. A similar approach was used by Høier & Marthinsen (1983) and Juretschke (1984).

(2) *Simple rule for phase determination*

If in an experiment the perpendicular-polarized component in the incident beam dominates, then from (23*a*) it is possible to derive a simple rule to determine

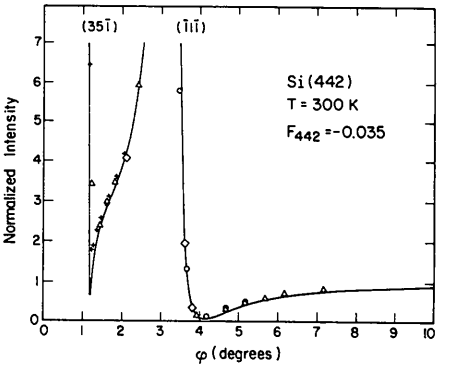

Fig. 5. Same as Fig. 3, except that the solid curves are calculated using equations (20) and (21), and the intensities are normalized to the two-beam value. $T=300$ K, $F_{442}=-0{\cdot}035$.

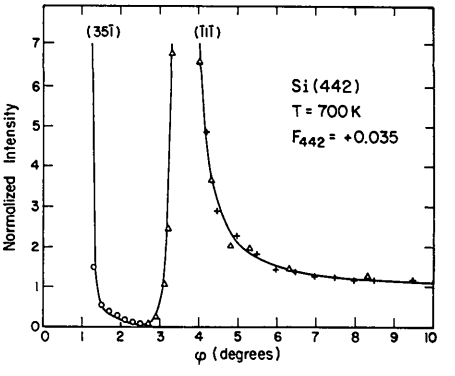

Fig. 6. Same as Fig. 5, except for: $T=700$ K, $F_{442}=+0{\cdot}035$.

the phases in a centrosymmetric crystal, as suggested by Chang (1982*a*).

Suppose that a crystal is orientated in such a way that **H** is the primary Bragg reflection. When the crystal rotates around **H**, the asymmetry in the intensity profile is observed near a three-beam point **L**. This asymmetry is due to the fact that the last term in (23*a*) possesses different signs on opposite sides of the excitation point. Since the numerator

$$k_L^2 - L_\sigma^2 = (k_0 + \mathbf{L}\cdot\hat{\mathbf{n}}_0)^2 + (\mathbf{L}\cdot\hat{\boldsymbol{\pi}}_0)^2 \geq 0,$$

the sign of this term is given by the sign of $\cos\delta_{HL}$ times the sign of $k_0^2 - k_L^2$, which is determined by whether **L** is inside or outside the Ewald sphere.

A quick way to obtain the sign of $k_0^2 - k_L^2$ is to look at an *Umweg* peak location plot of λ *versus* φ, the angle of rotation around **H**, near the three-beam point φ_L, as the one given in Fig. 7 for the Si 442-$\bar{1}1\bar{1}$ case. The wavelength used in an experiment is shown by a horizontal line $\lambda = \lambda_0$. Let $\lambda_L(\varphi)$ be the curve representing the node **L**. Then the position of **L** relative to the Ewald sphere is determined by whether $\lambda_L(\varphi)$ is above or below the line $\lambda = \lambda_0$ and whether **L** is on the larger or smaller portion of the Ewald sphere when $\varphi = \varphi_L$. By larger or smaller portion is meant one of the two portions separated by the plane that contains the primary reflection **H** and is perpendicular to the diffraction plane formed by $\mathbf{k}_0$ and **H**. We call it the *normal plane* for **H**. It is easy to see from equation (4) of the article by Cole, Chambers & Dunn (1962) that $L^2 - \mathbf{L}\cdot\mathbf{H}$ or $\mathbf{L}\cdot(\mathbf{L}-\mathbf{H})$ is the quantity that determines whether **L** is on the larger or smaller portion of the sphere: it is on the larger portion if $L^2 - \mathbf{L}\cdot\mathbf{H} > 0$ and on the smaller portion if $L^2 - \mathbf{L}\cdot\mathbf{H} < 0$. From simple geometrical arguments it is not difficult to obtain that in the case of $L^2 - \mathbf{L}\cdot\mathbf{H} > 0$, the node **L** is inside the Ewald sphere (hence $k_0^2 - k_L^2 > 0$) when $\lambda_L(\varphi)$ is above the horizontal line $\lambda = \lambda_0$ and is outside (hence $k_0^2 - k_L^2 < 0$) when $\lambda_L(\varphi)$ is below the line. The conclusion is reversed in the case of $L^2 - \mathbf{L}\cdot\mathbf{H} < 0$. The special case $L^2 - \mathbf{L}\cdot\mathbf{H} = 0$ means that both **L** and **H**−**L** are on the normal plane and on the Ewald sphere simultaneously, in which case no asymmetry effect exists, as will be discussed in the next section.

If we keep the same sense of rotation in experiments, we can state the rule to determine the sign of $\cos\delta_{HL}$ as follows: (i) In the case of $L^2 - \mathbf{L}\cdot\mathbf{H} > 0$: $\cos\delta_{HL} > 0$ if the observed intensity enhancement (reduction) and $\lambda_L > \lambda_0$ ($\lambda_L < \lambda_0$) occur at the same side of the three-beam point $\varphi = \varphi_L$; $\cos\delta_{HL} < 0$ if they occur at opposite sides of $\varphi = \varphi_L$. (ii) In the case of $L^2 - \mathbf{L}\cdot\mathbf{H} < 0$: the signs of $\cos\delta_{HL}$ in the above statements are reversed. For centrosymmetric crystals, we can further obtain that $\delta_{HL} = 0$ when $\cos\delta_{HL} > 0$ and $\delta_{HL} = \pi$ when $\cos\delta_{HL} < 0$.

Now let us apply this rule to the Si 442-$\bar{1}1\bar{1}$ experiment. Fig. 7 shows that $\lambda(\bar{1}1\bar{1})$ is above the dotted line, representing the wavelength used in the experiment, at the left side, and is below the dotted line at the right side of the three-beam point $\varphi \simeq 3°$. At $T = 300$ K, the experimental data in Fig. 3 show an intensity enhancement at left and a reduction at right. Since the quantity $L^2 - \mathbf{L}\cdot\mathbf{H} = 5 > 0$, from the rule stated above, it is easy to deduce that $\cos\delta_{HL} > 0$ and $\delta_{HL} = 0$. Since the phases $\alpha(\bar{1}1\bar{1}) = 0$ and $\alpha(533) = \pi$ are known, it is obvious that the phase of 442 has to be π: $\alpha(442) = \pi$. Similarly, at $T = 700$ K, Fig. 4 shows the intensity enhancement at right and the reduction at left, which yields $\cos\delta_{HL} < 0$ and $\delta_{HL} = \pi$, hence $\alpha(442) = 0$.

One should notice that the rule given above is essentially similar to the one given by Chang (1982*a*, *b*) except for the case $L^2 - \mathbf{L}\cdot\mathbf{H} < 0$. In fact, equation (14) for S_R, the sign of rotation, in the (1982*b*) reference is incomplete and should be replaced by the following:

$$S_R = S(\partial\lambda/\partial\varphi)\, S(L^2 - \mathbf{L}\cdot\mathbf{H}).$$

Here *S* stands for 'sign of', as used by Chang (1982*b*). The definition of S_L, the sign of the line profile, given in the (1982*a*) paper can then be used if one keeps the same sense of rotation around **H** between experiments and theory.

(3) *Pseudo-four-beam case* **O**, **H**, **L** *and* **H**−**L**

It has been observed by Schmidt (1986) in his experiment on V_3Si that the asymmetry effect disappears when both **L** and **H**−**L** go through the Ewald sphere simultaneously, even though these are strong reflections. This result has been verified using exact *n*-beam dynamical calculations. Similar results were also reported or discussed on other reflections of other crystals (Gong & Post, 1983; Kshevetskii, Mikhailyuk & Polyak, 1985). We can call it a *pseudo-four-beam* case since **L** and **H**−**L** are counted twice in the *n*-beam calculations and actually cancel out in contributing to the asymmetry effect.

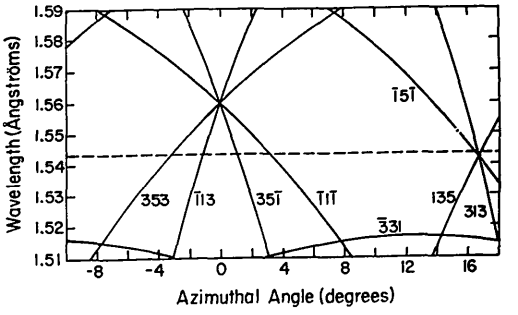

Fig. 7. *Umweganregung* peak location plot for the Si 442 experiment, as taken from Tischler *et al.* (1985). It shows the φ values of all possible *Umweg* reflections at any given wavelength λ. The zero on the φ axis corresponds to $\bar{1}10$ lying in the diffraction plane, mostly antiparallel to $\mathbf{k}_0$. The dotted horizontal line represents the wavelength used in the experiment (λ = 1·54335 Å).

This conclusion can be proved analytically using the present perturbation theory. For simplicity, we shall write (22) in units of $Nr_eF_H \exp(-ik_0r)/r$ and define $\gamma'_{HL} = \gamma_{HL} \exp(i\delta_{HL})$. Then, for the pseudo-four-beam case, (22) becomes

$$\mathbf{D} = \hat{\mathbf{n}} \times \left(\hat{\mathbf{n}} \times \left\{ \mathbf{D}_0 - \gamma'_{HL} \left[\frac{\mathbf{k}_L \times (\mathbf{k}_L \times \mathbf{D}_0)}{k_0^2 - k_L^2} + \frac{\mathbf{k}_{H-L} \times (\mathbf{k}_{H-L} \times \mathbf{D}_0)}{k_0^2 - k_{H-L}^2} \right] \right\} \right). \quad (24)$$

A necessary condition for $\mathbf{L}$ and $\mathbf{H}-\mathbf{L}$ to be on the Ewald sphere at the same time is that the plane containing $\mathbf{H}$ and $\mathbf{L}$ must be perpendicular to the diffraction plane formed by $\mathbf{k}_0$ and $k_0\hat{\mathbf{n}}$, so $\mathbf{k}_L$ and $\mathbf{k}_{H-L}$ can be decomposed into $\mathbf{k}_L = \mathbf{S}+\mathbf{R}$ and $\mathbf{k}_{H-L} = \mathbf{S}-\mathbf{R}$, with $\mathbf{S} \perp \mathbf{R}$, as shown in Fig. 8. When the crystal rotates infinitesimally around the scattering vector $\mathbf{H}$, the nodes $\mathbf{L}$ and $\mathbf{H}-\mathbf{L}$ deviate from the Ewald sphere by $\boldsymbol{\Delta}$ and $-\boldsymbol{\Delta}$ respectively. We denote the new $\mathbf{k}_L$ and $\mathbf{k}_{H-L}$ by $\mathbf{k}'_L$ and $\mathbf{k}'_{H-L}$, with $\mathbf{k}'_L = \mathbf{k}_L + \boldsymbol{\Delta}$ and $\mathbf{k}'_{H-L} = \mathbf{k}_{H-L} - \boldsymbol{\Delta}$. Hence, if we keep only the lowest-order non-vanishing terms, the denominators become

$$k_0^2 - k_L'^2 = k_0^2 - k_L^2 - 2\mathbf{k}_L \cdot \boldsymbol{\Delta} = -2S\Delta,$$

$$k_0^2 - k_{H-L}'^2 = k_0^2 - k_{H-L}^2 + 2\mathbf{k}_{H-L} \cdot \boldsymbol{\Delta} = 2S\Delta.$$

Therefore (24) becomes

$$\mathbf{D} = \hat{\mathbf{n}} \times \left[\hat{\mathbf{n}} \times \left(\mathbf{D}_0 + \gamma'_{HL} \frac{\mathbf{D}'}{2S\Delta} \right) \right],$$

where

$$\mathbf{D}' \equiv \mathbf{k}'_L \times (\mathbf{k}'_L \times \mathbf{D}_0) - \mathbf{k}'_{H-L} \times (\mathbf{k}'_{H-L} \times \mathbf{D}_0).$$

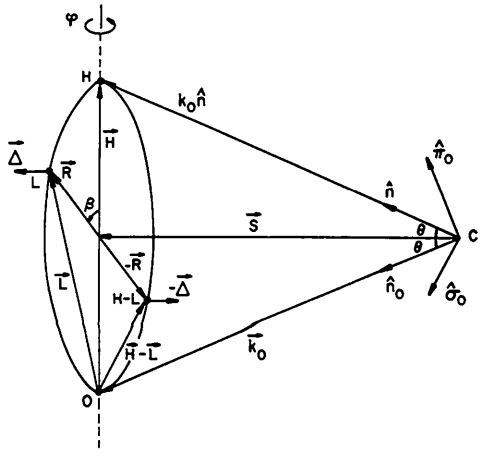

Fig. 8. A pseudo-four-beam case where both the secondary reflection $\mathbf{L}$ and the coupling reflection $\mathbf{H}-\mathbf{L}$ are on the Ewald sphere. The plane containing $\mathbf{H}$ and $\mathbf{L}$ is necessarily perpendicular to the diffraction plane formed by $\mathbf{k}_0$ and $k_0\hat{\mathbf{n}}$. The center of the Ewald sphere is at C. When the Ewald sphere rotates around $\mathbf{H}$, the nodes $\mathbf{L}$ and $\mathbf{H}-\mathbf{L}$ deviate from the sphere by $\boldsymbol{\Delta}$ and $-\boldsymbol{\Delta}$ respectively. $\hat{\mathbf{n}}_0$ is a unit vector along $\mathbf{k}_0$, $\hat{\boldsymbol{\sigma}}_0$ is a unit vector normal to the diffraction plane and $\hat{\boldsymbol{\pi}}_0 = \hat{\mathbf{n}}_0 \times \hat{\boldsymbol{\sigma}}_0$.

To evaluate $\mathbf{D}'$, we again keep only the lowest-order non-zero terms, which turn out to be the zeroth order in Δ. Hence

$$\mathbf{D}' = (\mathbf{S}+\mathbf{R}) \times [(\mathbf{S}+\mathbf{R}) \times \mathbf{D}_0] - (\mathbf{S}-\mathbf{R}) \times [(\mathbf{S}-\mathbf{R}) \times \mathbf{D}_0],$$

which can be simplified further to

$$\mathbf{D}' = 2[\mathbf{R}(\mathbf{S} \cdot \mathbf{D}_0) + \mathbf{S}(\mathbf{R} \cdot \mathbf{D}_0)].$$

With the help of Fig. 8, we write that, for a perpendicular polarization $\mathbf{D}_0 = \hat{\boldsymbol{\sigma}}_0$,

$$\mathbf{D}' = 2RS \sin\beta,$$

$$\hat{\mathbf{n}} \times (\hat{\mathbf{n}} \times \mathbf{D}') = \hat{\boldsymbol{\pi}} 2RS \sin\beta \sin\theta.$$

Hence the diffracted wave field becomes

$$\mathbf{D}_\perp = -\hat{\boldsymbol{\sigma}} + \gamma'_{HL}(R \sin\beta \sin\theta/\Delta)\hat{\boldsymbol{\pi}},$$

and the intensity

$$I_\perp = 1 + |\gamma'_{HL}|^2 (R \sin\beta \sin\theta/\Delta)^2. \quad (25a)$$

Similarly, for a parallel polarization $\mathbf{D}_0 = \hat{\boldsymbol{\pi}}_0$,

$$\mathbf{D}' = 2(RS \cos\beta \cos\theta + SR \sin\theta),$$

$$\hat{\mathbf{n}} \times (\hat{\mathbf{n}} \times \mathbf{D}') = -\hat{\boldsymbol{\sigma}} 2RS \sin\beta \sin\theta.$$

Hence

$$\mathbf{D}_\parallel = -\hat{\boldsymbol{\pi}} \cos 2\theta - \gamma'_{HL}(R \sin\beta \sin\theta/\Delta)\hat{\boldsymbol{\sigma}},$$

$$I_\parallel = \cos^2 2\theta + |\gamma'_{HL}|^2 (R \sin\beta \sin\theta/\Delta)^2. \quad (25b)$$

Since only Δ^2 terms appear in (25), we conclude that there are no asymmetry effects in the pseudo-four-beam case for common X-ray sources (*e.g.* unpolarized or perpendicularly polarized). Therefore, for a phase determination experiment, one should avoid the pseudo-four-beam case.

Concluding remarks

The perturbation theory of scattering in electrodynamics can be used to obtain a simple analytical expression for the diffracted X-ray wave field from a crystal that includes the effects of multibeam perturbations on the conventional two-beam wavefield, without having to solve the eigen equation for the multibeams. Although it cannot be applied to the center of a multiple reflection peak, it allows one to do fast and fairly accurate calculations near a multibeam point and shows explicitly the asymmetric structure in the intensity and its phase dependence when a third reciprocal-lattice point moves across the Ewald sphere, which makes it possible to obtain a simple rule for phase determination in centrosymmetric crystals. The fact that this approach is kinematic in nature shows that multibeam effects can be treated within a single-scattering framework and phase information can be preserved in kinematic theory much in the same way as in dynamical theory.

It also proves that the asymmetry effect around a multibeam point is intrinsically due to interference among different Bragg waves and its existence does not depend on absorption, refraction, diffraction geometry, crystal shape and boundary conditions. The good agreement between the present theory and the Si 442 experimental data, as well as the exact n-beam dynamical calculations, indicates the validity of the perturbational approach, at least in the weak-scattering regime. It is hoped that more experimental and theoretical investigations may be generated in the future in the area of multibeam diffraction effects and the phase problem in X-ray crystallography.

The author is grateful to Professor R. Colella for many enlightening discussions and his encouragement to publish this article. The author would also like to thank the referees for their helpful suggestions and comments. This work is supported by the National Science Foundation under Grant No. DMR-8402174, and is based on research performed as partial fulfilment of the requirements for the author's PhD degree in physics at Purdue University.

References

BATTERMAN, B. W. & COLE, H. (1964). *Rev. Mod. Phys.* **36**, 681-717.
CHANG, S. L. (1982*a*). *Phys. Rev. Lett.* **48**, 163-166.
CHANG, S. L. (1982*b*). *Acta Cryst.* A**38**, 516-521.
CHAPMAN, L. D., YODER, D. R. & COLELLA, R. (1981). *Phys. Rev. Lett.* **46**, 1578-1581.
COLE, H., CHAMBERS, F. W. & DUNN, H. M. (1962). *Acta Cryst.* **15**, 138-144.
COLELLA, R. (1974). *Acta Cryst.* A**30**, 413-423.
GONG, P. P. & POST, B. (1983). *Acta Cryst.* A**39**, 719-724.
HØIER, R. & MARTHINSEN, K. (1983). *Acta Cryst.* A**39**, 854-860.
HÜMMER, K. & BILLY, H. (1986). *Acta Cryst.* A**42**, 127-133.
JACKSON, J. D. (1974). *Classical Electrodynamics*, 2nd ed., pp. 418-421. New York: John Wiley.
JURETSCHKE, H. J. (1982). *Phys. Rev. Lett.* **48**, 1487-1489.
JURETSCHKE, H. J. (1984). *Acta Cryst.* A**40**, 379-389.
KSHEVETSKII, S. A., MIKHAILYUK, I. P. & POLYAK, M. I. (1985). *Sov. Phys. Crystallogr.* **30**, 145-147.
POST, B. (1977). *Phys. Rev. Lett.* **39**, 760-763.
SCHIFF, L. I. (1955). *Quantum Mechanics*, 2nd ed., pp. 163-164. New York: McGraw-Hill.
SCHMIDT, M. C. (1986). PhD Thesis, Purdue Univ.
SCHMIDT, M. C. & COLELLA, R. (1985). *Phys. Rev. Lett.* **55**, 715-717.
TISCHLER, J. Z., SHEN, Q. & COLELLA, R. (1985). *Acta Cryst.* A**41**, 451-453.
WARREN, B. E. (1969). *X-ray Diffraction*, pp. 29, 41. New York: Addison Wesley.

Acta Cryst. (1986). A**42**, 533-538

The Current Status of Phase Determination by Means of Multiple Bragg Diffraction

BY Q. SHEN AND R. COLELLA

Physics Department, Purdue University, West Lafayette, Indiana 47907, *USA*

(*Received* 11 *March* 1986; *accepted* 27 *May* 1986)

Abstract

The feasibility of multibeam diffraction for determining phases of structure factors is assessed on the basis of recent contributions and experiments in progress. It is shown that the method works well in situations in which the global interaction between X-ray photons and the crystal is weak, in which case diffraction takes place by single scattering events, and crystal perfection does not play a role in interpreting the experimental results. Two successful examples of phase determinations using the notion of virtual Bragg scattering are presented. One case is of particular interest, because the crystal (V_3Si) is mosaic, and the phases were *a priori* unknown. Some problems and limitations of the method are encountered when trying to extend this technique to organic crystals of relatively large cell size, with spherical or irregular shape. Some data and calculations are presented for benzil, $C_{14}H_{10}O_2$, a crystal isomorphous with quartz. It is concluded that the resolution presently available from standard laboratory set-ups is not adequate for application of this method to a crystal like benzil, but that use of synchrotron radiation beams will probably remove these obstacles.

1. Introduction

It is indeed a pleasure to write a paper dealing with multiple-beam diffraction for this issue of *Acta Crystallographica*, because this was in fact a topic in which Paul Ewald had a special interest. The last two of Ewald's papers in *Acta* are precisely on this subject (Ewald & Héno, 1968; Héno & Ewald, 1968) and it is fitting to make reference here to these two papers and appreciate the progress made during the last eighteen years.

There has been, recently, a renewed interest in the idea of using multiple Bragg scattering for extracting

0108-7673/86/060533-06$01.50